research articles Journal of proteome research

Lysosomal Membranes from Beige Mice Contain Higher Than Normal Levels of Endoplasmic Reticulum Proteins

Huiwen Zhang,[†] Xiaolian Fan,[†] Richard D. Bagshaw,[†] Li Zhang,[†] Don J. Mahuran,[†,‡] and John W. Callahan*[,†,§,∥]

Research Institute, The Hospital for Sick Children, Toronto, Ontario M5G 1X8, Canada, and Departments of Laboratory Medicine and Pathobiology, Biochemistry, and Pediatrics, University of Toronto, Toronto, Ontario M5S 1A8, Canada

Received August 11, 2006

Chediak−Higashi syndrome is characterized by dysfunctional giant organelles of common origin, that is, lysosomes, melanosomes, and platelet dense bodies. Its defective gene *LYST* encodes a large molecular weight protein whose function is unknown. The Beige mouse also defective in Lyst is a good model of the human disease. Purified lysosomes from Beige and normal black mouse livers were used to carry out a proteomics study. Two-dimensional gel electrophoretic separation of soluble lysosomal proteins of Beige and normal mice revealed no major differences. The cleavable isotope-coded affinity tag (cICAT) technique was used to compare the composition of Beige and normal lysosomal membrane proteins. While the levels of common proteins, that is, Lamp1, Lamp2, and Niemann-Pick type C1, were decreased in Beige mice, there was an increase in the levels of endoplasmic reticulum (ER) resident proteins, for example, cytochrome P450, NADPH-cytochrome P450 oxidoreductase, and flavin-containing monooxygenase. Confocal microscopy confirmed that another ER protein, calnexin, colocalizes with Lamp1 on membranes of giant lysosomes from fibroblasts of Chediak−Higashi syndrome patient. Our results suggest that LYST may play a role in either preventing inappropriate incorporation of proteins into the lysosomal membrane or in membrane recycling/maturation.

Keywords: organelle proteomics • lysosomal membrane • Chediak−Higashi • cleavable isotope-coded affinity tag

Introduction

The Chediak−Higashi syndrome (CHS) is a rare autosomal recessive disorder of humans. Homologous diseases have been found in other species, that is, mouse (named Beige), rat, mink, cat, cattle, and killer whales.[1] Clinically, CHS/Beige are characterized by severe immunologic defects with recurrent severe infections, partial albinism, and a mild bleeding tendency. Some patients progress to a lethal accelerated phase that is correlated with EBV infection. Bone marrow transplantation is the only treatment for this disease. At the cellular level, CHS patients are distinguished by juxtanuclear giant dense organelles in all cell types, including melanosomes in melanocytes, dense bodies in platelets, secretory lysosomes in hematopoietic cells, and conventional lysosomes in other cell types. Histochemical and immunofluorescence studies have shown the giant dense organelles in both CHS and Beige were positive for marker proteins of late endosomes and lysosomes, for example, cathepsin D, lysosome-associated membrane protein (Lamp) 1, Lamp 2, and a 120-kDa lysosomal glycoprotein, while negative for mannose-6-phosphate receptor.[2,3] BSA or colloidal gold was transported to the giant organelles but required much longer chase times, suggesting some impairment in fluid-phase endocytosis. However, beta 2-macroglobulin was taken up and degraded at an apparently normal rate by both CHS or Beige cells, suggesting no abnormalities in receptor-mediated endocytosis.[3] Additionally, no significant endogenous intracellular protein degradation defect was observed in Beige mouse fibroblasts.[4]

The gene responsible for human CHS, encodes the LYST (*Lys*osomal *T*rafficking Regulator) protein, with molecular weight of 430 kDa, which is highly conserved in all species.[5] It has 87.9% amino acid identity with the mouse homologue.[6] LYST protein belongs to a large family of proteins characterized by the presence of a BEACH (*Be*ige and *C*hediak−*H*igashi Syndrome) and several WD domains in its C-terminal region. To date, the exact *in vivo* function of LYST and its BEACH domain remain poorly understood. Two members of the Beige/CHS (BEACH) family in *Dictyostelium* have been reported to be involved at different stages of the endocytic pathway.[7,8] Alfy, a protein containing a FYVE domain, as well as a BEACH domain, associates with protein granules and autophagic membranes.[9] LYST has been localized to the cytosol[5] and also

* Corresponding author. John W. Callahan, Ph.D., The Hospital for Sick Children, Research Institute, Elm Wing, Room 9144, 555 University Avenue, Toronto M5G 1X8. Phone, 416-813-5754; fax, 426-813-8700; e-mail, john.callahan@sickkids.ca.

[†] Research Institute, The Hospital for Sick Children.

[‡] Department of Laboratory Medicine and Pathobiology, University of Toronto..

[§] Department of Biochemistry, University of Toronto.

[∥] Department of Pediatrics, University of Toronto.

10.1021/pr060407o CCC: $37.00
Published on Web 12/14/2006

has been found associated with a punctate staining pattern in the cell, partially aligned along microtubules.[10] The high molecular weight makes conventional methods of studying protein structure−function less applicable to LYST. A proteomics study of the hallmark of LYST-deficiency, that is, "giant lysosomes", is likely to help elucidate the *in vivo* function of this large cytosolic protein.

In this study, we have taken a proteomics approach to compare the lysosomal protein composition of Beige mice with that of normal black mice in order to develop new insights into the function of the LYST protein.

Experimental Section

1. Animals and Cells. C57BL/J and C57BL/J-Lyst were purchased from Jackson Laboratories. Chediak−Higashi Syndrome patient and normal human fibroblasts were maintained in Dulbecco's modified Eagle's medium (HyClone) supplemented with 10% fetal bovine serum (Sigma) at 37 °C in 5% CO_2 with antibiotics. Cultures were used between passage numbers 3−20.

2. Antibodies. Antibodies used were rabbit polyclonal anti-calnexin N-terminal (sc-11397, Santa Cruz Biotechnology), rat monoclonal anti-mouse Lamp2 (GL2A7), mouse monoclonal anti-human Lamp1 (H4A3, Developmental Studies Hybridoma Bank at University of Iowa), and anti-Nicastrin (Affinity Bioreagents). A rabbit β-glucosidase antibody was raised against cerezyme, from Genzyme Corp. in our lab. Polyclonal antibodies to Sec61-α and -β were a generous gift from Dr. Richard Zimmermann (Universitat des Saarlandes, Germany).

3. Percoll-Gradient Isolation of a Subcellular Fractionation Highly Enriched in Lysosomes. Fresh mouse livers were minced with scissors, suspended in cold (all procedures were done at 4 °C unless noted otherwise) 0.25 M sucrose, containing proteinase inhibitors (1 mg/mL Pepstatin A, 1 mg/mL Leupeptin, and 1 mM PMSF), and homogenized with a Thomas homogenizer for 8 strokes at 100 rpm (Supplementary Figure 1 in Supporting Information). Homogenates were centrifuged at 1000*g* for 10 min. The postnuclear supernatant (PNS) was adjusted to 1 mM $CaCl_2$ and incubated at 37 °C for 5 min, and the crude organelles were collected after centrifugation at 15 000*g* for 15 min. The resulting supernatant was centrifuged at 100 000*g* for 1 h to collect the microsome fraction and a final supernatant. The crude organelle pellet was resuspended in 0.25 M sucrose, and crude organelles (1.5 mL) were then loaded onto 8 mL of 40% Percoll in a sealable centrifuge tube. These were centrifuged in a 50 Ti Beckman rotor at 60 000*g* for 45 min. Fractions were collected from the bottom of the tube in the following volumes: fractions 1−5 (0.5 mL), 6−7 (1.0 mL), and 8 (1.5 mL). Each fraction was underloaded with a 0.2 mL 50% (w/v) sucrose cushion and centrifuged at 300 000*g* for 1 h in a Beckman TL 100.3 rotor. Lysosomes at the interface were collected and resuspended in 0.25 M sucrose, and the resultant sample was collected by centrifugation at 25 000*g* for 20 min. Each fraction was analyzed using 10% SDS-PAGE and Western blotting.[11] Hexosaminidase activity was assayed as described.[12] Protein was measured by the BCA method (Pierce) with bovine serum albumin fraction V (Pierce) as a standard. Lysosomes were subfractionated into soluble, membrane-associated, and integral membrane fractions as described previously.[13]

4. Two-Dimensional Gel Electrophoresis. The proteins contained in the soluble fraction were desalted by spin dialysis with a Millipore centrifugal filter. Dialysis buffer consisted of 7 M urea, 2 M thiourea, and 2% CHAPS. After changing the dialysis buffer four times, DTT and IPG (Amersham Pharmacia) were added to 100 mM and 2%, respectively, to each sample, as well as a few crystals of bromophenol blue. IPG strips, 18 cm long, with a nonlinear pH 3−10 range, were used. After overnight rehydration, the first IEF dimensional separation was accomplished on a IPGPhor apparatus (Amersham Pharmacia) for a total of 60 000 Vhr. Before the second dimensional separation, strips were equilibrated in two steps. first with 125 mM DTT in equilibration buffer (50 mM Tris-HCl, pH 8.0, 6 M urea, 30% (w/v) glycerol, and 2% (w/v) SDS), and then with 125 mM Iodoacetamide in the same equilibration buffer. The second dimensional separation was performed on a 1 mm thick, 18.3 cm × 19.3 cm 10% polyacrylamide gel (Protein XL vertical electrophoresis cells, Bio-Rad). Proteins were revealed by either silver nitrate or colloidal blue staining.[14]

5. Ion Trap Mass Spectrometry Analysis of Spots on 2-D Gels. Silver nitrate-stained protein spots from the soluble fraction of lysosomes from normal black mice were cut from the gel, destained with 15 mM potassium ferricyanide and 50 mM sodium thiosulfate, and then processed for in-gel digestion with trypsin as described previously.[15] Recovered peptides were subjected to an Agilent 1100 nanoflow HPLC separation and Thermo LCQ Deca XP ion trap mass spectrometric analysis. Peptide hits were searched using MS/MS ion search (MASCOT, www.matrixscience.com) from the National Center for Biotechnology nonredundant protein (NCBI nr) database. Database search criteria included peptide tolerance of 0.8 Da, MS/MS tolerance of 0.8 Da, and 2 possible missed cleavage sites. All proteins identified were confirmed manually.

6. cICAT Analysis of Lysosomal Membrane Proteins. The cleavable ICAT (cICAT) kit was obtained from ABI (CA). Procedures were carried out according to their protocol. Briefly, lysosomal integral membrane protein fractions were denatured in 6 M urea, 1% (w/v) octyl-beta-glucopyranoside, 50 mM Tris (pH 8.5), and 0.1% (w/v) SDS and sonicated for 1 h in a 4 °C water bath. The samples were centrifuged at 13 000 rpm for 10 min. The supernatants were used for cICAT labeling. First the protein concentration of each sample was determined by the BCA method. The TECP reducing reagent was added to a 100 μg sample to a final concentration of 2 mM. Beige and normal black mouse lysosomal membrane proteins were boiled separately for 10 min before being labeled with either the isotopically heavy (^{13}C) or light (^{12}C) cleavable ICAT reagent, respectively. DTT was added to 12 mM, and the samples were allowed to stand for 5 min at room temperature. The samples were diluted to 1.25 mM with 50 mM Tris (pH 8.5) and 0.1% SDS before samples were combined and digested using sequence grade trypsin (25 μg/mL) overnight at 37 °C. The trypsinized samples were adjusted to pH ∼3 and subdivided into 10, 100, and 350 mM KCl fractions sequentially by the cation-exchange cartridge. cICAT-labeled peptides were then neutralized and passed over the avidin cartridge. Unlabeled peptides (those not containing a cysteine) remained unbound. The labeled peptides were dried under centrifugal vacuum, resuspended in 90 μL cleaving reagent, and then incubated at 37°C for 2 h. Cleaved samples were dried and resuspended in 0.1% TFA for analysis by LC−ESI−MS/MS.

7. Liquid Chromatography and Mass Spectrometry. Reverse-phase chromatographic separation was performed in an on-line Waters CapLC capillary HPLC system (Waters, Milford, MA). Samples were first loaded onto a precolumn (300 μm i.d. × 5 mm), packed with C18 PepMap100 (5 μm particle size, 100 Å pore size silica), and then eluted to an analytical column for

further separation. The analytical column had dimensions of 75 μm i.d. × 15 cm, packed with C18 PepMap100 (3 μm particle size, 100 Å pore size silica). Both columns were manufactured by LC Packings (Amsterdam, The Netherlands). The mobile phase was composed of solutions A and B, where A was water with 0.1% formic acid and B was acetonitrile with 0.1% formic acid. The gradient started at 5% B and ramped to 80% B in 55 min. Flow rate was estimated to be 200 nL/min, which was achieved by splitting the mixture of A and B right before they were delivered to the columns. Mass spectrometry was performed on a QSTAR XL hybrid quadrupole time-of-flight mass spectrometer (Applied Biosystems/MDS Sciex, Concord, ON, Canada) using Information Dependent Acquisition with each cycle time of 7 s (1 s MS scan followed by three 2 s MS/MS scans).

Peptide quantification was analyzed by ProICAT (ABI) against an Interrogator Algorithm Search Database created using a mouse protein FASTA database (downloaded on November, 2005 from NCBI's ftp site, ftp://ftp.ncbi.nlm.nih.gov/genomes/M_musculus/protein/). A preset modification, the oxidation of methionine residues, is built into the Interrogator search database, while acetyl, deamidation, and pyroglutamic acid modifications were set in the "Zone modification search". Peptides with confidence above 85% were regarded as hits. The raw data also were analyzed using MS/MS ion search according to Mascot (www.matrixscience.com) as decribed earlier.[13] Peptide tolerance and MS/MS tolerance was set to 0.2 Da.

8. SDS-PAGE and Immunoblots. Equal amounts of proteins (40 μg) from different samples were separated by mini SDS-PAGE and transferred to nitrocellulose. Primary antibodies are shown in the respective figures. Detection was done using species-appropriate horseradish peroxidase-conjugated secondary antibodies with ECL and Hyperfilm (Amersham Biosciences).

9. Immunofluorescence. Cells were loaded with tetramethylrhodamine dextran (Invitrogen) overnight and chased for 3 h, then fixed with 4% paraformaldehyde at 37 °C for 20 min. After being washed twice with PBS, cells were permeabilized/blocked by treatment with 0.2% saponin (Calbiochem) containing 10% normal goat serum (SS-PBS) for 30 min. Primary and secondary antibodies were overlaid on coverslips in SS-PBS for 1 h and 30 min separately, followed by three washes with PBS. Coverslips were mounted onto 1-mm glass sides using fluorescent mounting medium (DakoCytomation, Canada). Samples were analyzed using a Zeiss Axiovert confocal microscope (63× objective).

10. Transmission Electron Microscopy. Lysosomal pellets were fixed in 3.2% paraformaldehyde and 2.5% glutaraldehyde in Sorensen's phosphate buffer for 1 h at room temperature. After three washes with Sorensen's phosphate buffer, they were postfixed with 2% OsO_4 in Sorensen's phosphate buffer for 2 h at room temperature in the dark and washed with Sorensen's phosphate buffer another three times. Lysosomal pellets were dehydrated in ascending series of ethanol and infiltrated with a graded series of Epon Araldite and propylene oxide mixtures. Following polymerization, ultrathin sections were prepared with a diamond knife on an ultramicrotome and mounted on grids. Sections were then stained with saturated ethanolic uranyl acetate and lead citrate prior to examination and photography in a Hitachi H7000 transmission electron microscope at an accelerating voltage of 75kV.

Table 1. Lysosome Purification by Percoll

	activity ((μmol/h)/mg)		yield (%)		purification (-fold)[a]	
fraction	N	Bg	N	Bg	N	Bg
Homogenate	1.7	1.76	100	100	1	1
Post Nuclear Supernatant	1.0	0.85	32	40	1	1
Crude Organelles	2.8	2.8	24	15	2.7	3.3
Fraction 2	77.7	75.8	2.8	0.8	77	89
Fraction 3	37.5	53.7	1.8	0.6	37	63

[a] The postnuclear supernatant specific activity was taken as the starting point for the lysosome purification and was set to 1.0.

Results and Discussion

Percoll Is an Efficient Method To Isolate Lysosomes from Mouse Liver. Using a $CaCl_2$ treatment to swell mitochondria before loading the crude organelles onto Percoll, we obtained highly purified lysosomes, as judged by the high level of enrichment in the specific activity of total lysosomal β-hexosaminidase (Table 1). The degree of enrichment was 72 ± 17-fold ($n = 4$) for normal mice and 66 ± 16-fold ($n = 4$) for the Beige mice, levels comparable to others.[16] The bulk of the lysosomes (Figure 1A), as judged by hexosaminidase activity (Figure 1B), appeared in fractions 2 and 3, while the majority of the total protein (Figure 1B) was found in the upper part of the gradient (fraction 6−8). Samples from comparable preparations were pooled for proteomic analysis. Western blot analysis, with Lamp1 and Nicastrin antibodies, was used to confirm the purity of the lysosomal fraction (Figure 1C). The 49 kDa subunit of complex I was used as a marker of mitochondria and was observed primarily in fractions 6 and 7. Similarly, the same fractions contained the majority of the rough ER protein (sec61-α and -β), while the Golgi protein gpp130 was detected only in fraction 8.

Regular transmission electron microscopy was used to compare (at the same levels of magnification) the lysosomal fractions from Beige and normal black mouse livers (Figure 2). Most of the observable structures were secondary lysosomes based on the occurrence of high-density particles in the matrix and autophagosomes undergoing fusion with lysosomes (appearing like a white cyst attached to a black body). Further, as expected, Beige lysosomes were larger with a diameter up to 1 μm, while normal mouse lysosomes had an average diameter of 0.5 μm. We were unable to discern mitochondrial elements such as the cristae of the inner membrane or ribosome-studded membranes of the rough ER, cellular components with approximately the same buoyant density as lysosomes. Thus, with the Percoll method of purification, we isolated representative populations of lysosomes that reflect the size difference between the Beige and normal liver lysosomes with a minimum of contamination from other cellular organelles.

Analysis of the Soluble Protein Components from the Beige and Normal Liver Lysosomal Fractions. Freeze/thaw disruption of the lysosomes produces a soluble and a membrane fraction as expected.[13] The soluble proteins from the lysosomal fractions of Beige and normal mouse liver were resolved by two-dimensional electrophoresis and visualized by silver nitrate (Supplementary Figure 2A,2B in Supporting Information) or colloidal blue (Supplementary Figure 2C,D in Supporting Information). Virtually every spot in Beige (Supplementary Figure 2A,C in Supporting Information) had its corresponding spot in normal black mouse samples (Supplementary Figure

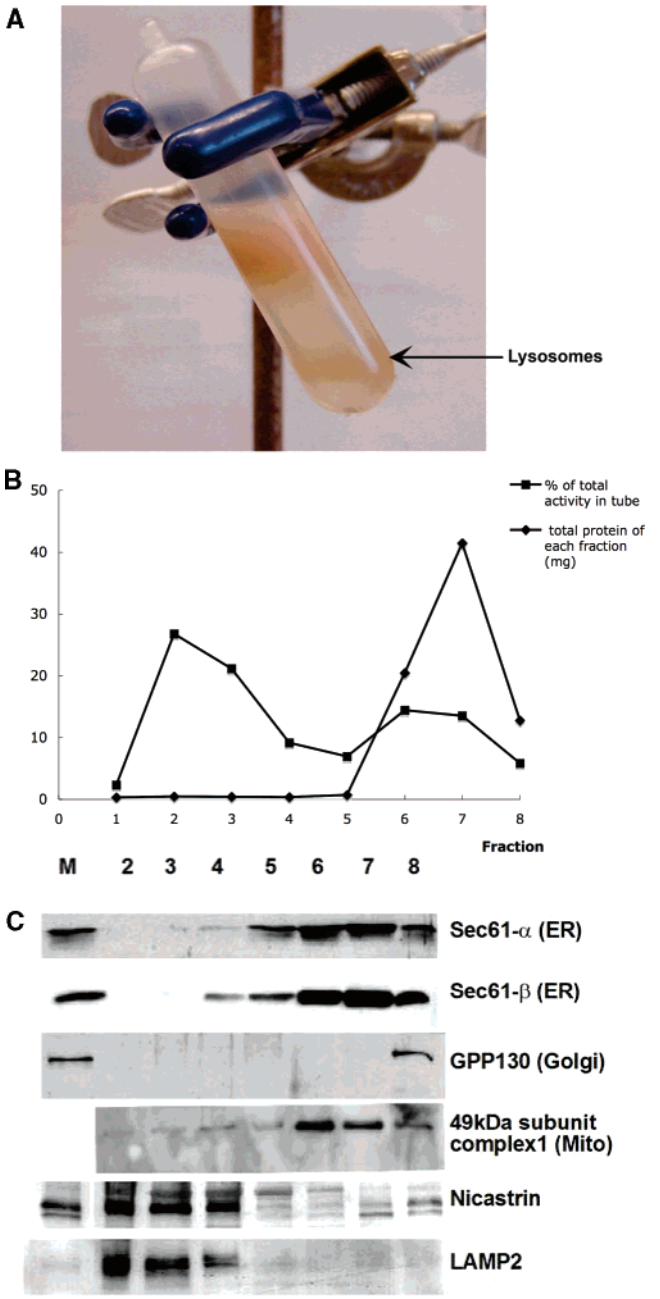

Figure 1. Characterization of mouse liver lysosomes. (A) Percoll density gradient separation of lysosomes (brown colored organelles near the bottom of tube). (B) Assay results from fractions collected from the bottom of the tube shown in panel A. Lysosomal hexosaminidase activity is concentrated in fractions 2 and 3, well away from the vast majority of protein found in fractions 6−8. (C) Western blot analyses of the fractions from panel A. The lysosomal fractions 2 and 3 identified by enzyme and protein assays, in panel B, are shown to contain lysosomal markers Lamp 2 and Nicastrin, but negligible amounts of the rough ER protein sec61-α and -β, the mitochondrial protein 49 kDa subunit of complex 1, and no Golgi protein gpp130.

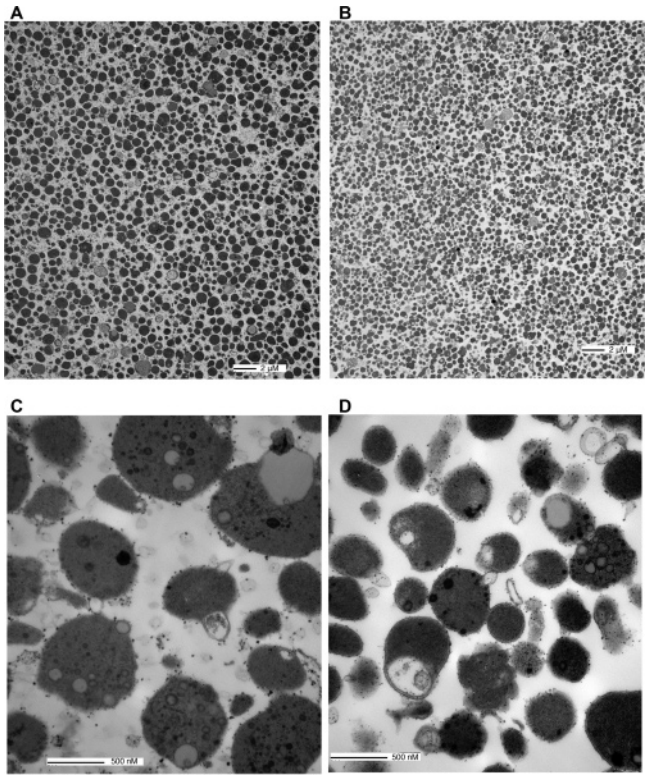

Figure 2. Electron microscopic analysis of lysosomal preparations. Lysosomes (fractions 2 and 3, Figure 2) from Beige (A and C) and normal (B and D) mice were examined as described in Experimental Section. Low magnification, 4000× (A and B), reveals that nearly all the organelles are recognizably lysosomes and that Beige lysosomes are generally larger in diameter than normal lysosomes. At high magnification, 40 000× (C and D), characteristic lysosome and autophagolysosome structures can be seen with the diameters of lysosomes from Beige mice being twice that of lysosomes from normal mice.

2B,D in Supporting Information). In total, 177 spots were cut from the gel of normal black mouse lysosomes (Supplementary Figure 2B in Supporting Information). On the basis of ion trap MS/MS, we identified 90 proteins in this fraction (Supplementary Table 1 in Supporting Information). These were subgrouped into 6 classes, that is, 16 cathepsins, 13 glycosidases, 4 sulfatases, 16 proteins involved in lipid metabolism, and 23 related to other lysosomal functions. The remaining 17 proteins, largely ribosomal constitutional proteins and mitochondrial proteins, may be considered as minor contaminants or proteins awaiting degradation. In the isolation method, we did not use harsh reagents, such as a high salt concentration, to dissociate ribosomes from the rough ER. Significantly, while the soluble ribosome constitutional proteins that were identified were represented by only 1 or 2 identifiable peptides, most lysosomal proteins were represented by 5 or more identifiable peptides. These data further demonstrate the low level of RER/ER contamination in our lysosomal fraction. Three proteins, mammalian ependymin-related protein 2, retinoid-inducible serine carboxypeptidase, and a hypothetical 66.3 kDa protein (similar to laminin A), have been previously identified as novel, soluble lysosomal proteins.[17] One spot from the Beige lysosomal fraction (Supplementary Figure 2C in Supporting Information, marked by an arrow) did have a stronger signal than the corresponding spot from the normal lysosomal fraction (Supplementary Figure 2D in Supporting Information). It was identified as ERp57 by ion trap MS/MS.

Comparison of the Membrane Protein Components of Beige and Normal Mouse Liver Lysosomes. The protein components of the lysosomal membrane fractions were identified and quantified by ProICAT (ABI). All of the peptides used to identify these proteins contained a labeled cysteine and

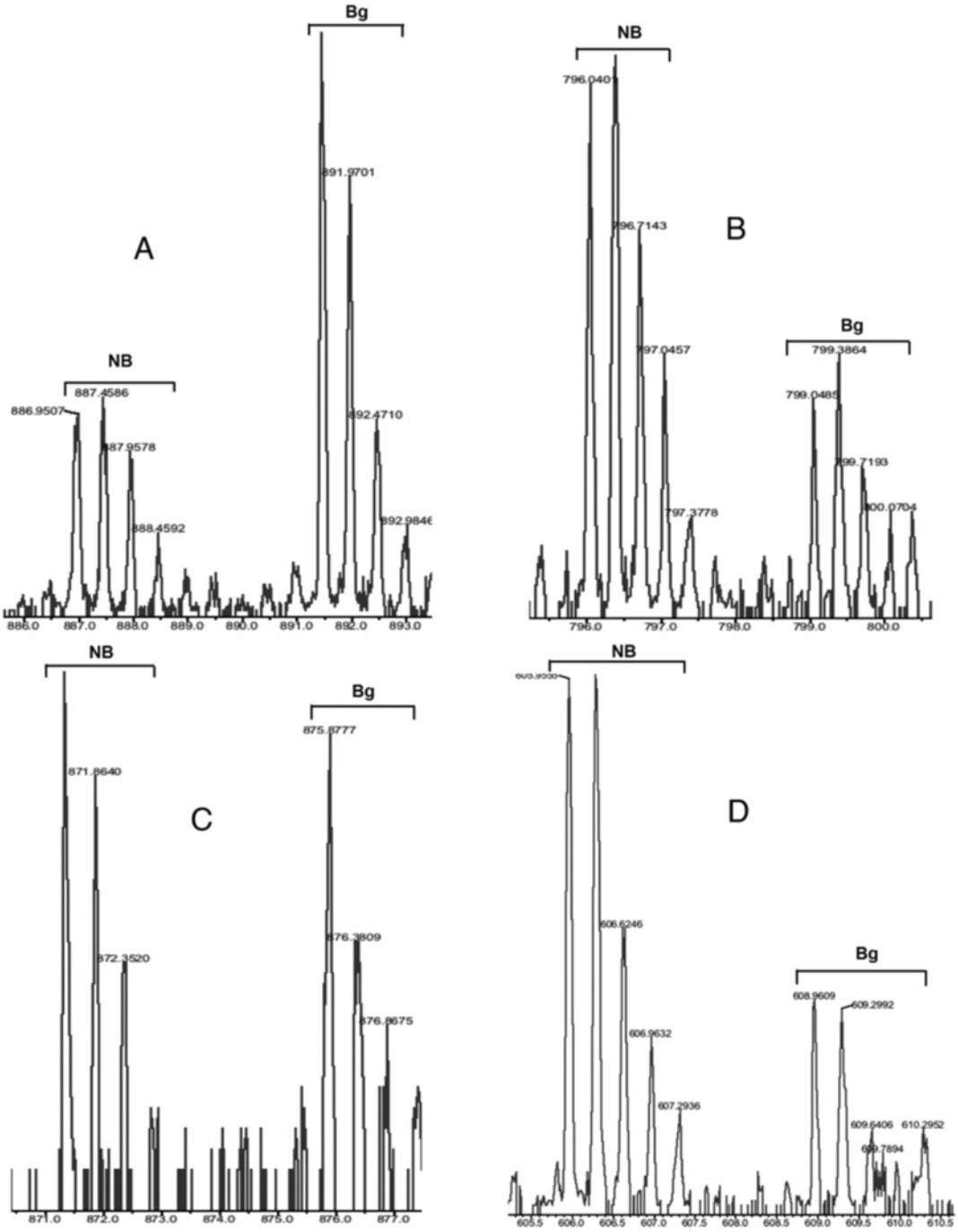

Figure 3. Representative mass spectrum peptide pairs of Beige and normal lysosomal membrane proteins. Beige (Bg) and normal (NB) lysosomal membrane proteins were separately labeled with isotopically heavy (^{13}C) and light (^{12}C) cleavable ICAT reagent, respectively, and mixed prior to analysis. Panel A is a peptide pair from cytochrome P450 2c29, a conventional ER protein; panel B is Lamp2, a common lysosome membrane protein; panel C is legumain, a soluble lysosome protein; panel D is the lysosomal membrane protein Nicastrin.

appeared as pairs of heavy and light labels from Beige and normal lysosomal membranes, respectively (Figure 3). In total, 111 proteins in the lysosomal membrane fraction were identified and quantified by ProICAT (ABI), of which more than 60% were predicted to have transmembrane domains by TMHMM and/or TMPRED (Table 2 and Supplementary Table 2 in Supporting Information). The proteins included the well-known lysosomal membrane proteins, Lamp1, Lamp2, NPC 1, vacuolar proton-translocating ATPase 100 kDa subunit isoforms a1 and a3, mucolipin 1,[18] spinster,[19] proton-coupled divalent metal ion transporters, Flotillins 1 and 2, dipeptidylpeptidase IV, and sialin.[20] It has previously been reported that the activities of two lysosomal enzymes, neutrophil elastase and cathepsin G, are decreased in CHS patients and Beige mice. The intracellular forms of these enzymes are membrane-bound.[21,22] Neither of these was found in the soluble fraction, but we detected neutrophil elastase in the integral membrane fraction. In the Beige membrane fraction, neutrophil elastase was significantly decreased (~21% of normal) compared to its level in the normal sample. This result is comparable to a previously published

Table 2. Proteins Identified in the Lysosomal Membrane Were Classified According to Their Subcellular Compartmentalization

Entrez number	protein name	ratio (Bg/NB)	additional information
Lysosome/Late Endosome			
27370146	solute carrier family 17, member 5 (sialin)	0.16	
7657060	neutrophil elastase	0.21	
6679054	myeloid bactenecin (F1, neutrophilic granule protein)	0.35	
29145014	Lamp1	0.40	
17512334	natural resistance-associated macrophage protein 2(SLC11A2, proton-coupled divalent metal ion transporters)	0.41	
31981205	nicastrin	0.41	
15029719	vacuolar adenosine triphosphatase subunit D	0.48	
26347041	Lamp2	0.49	
4206090	snapin	0.50	
71060007	lactotransferrin	0.50	
6679104	Niemann Pick type C1	0.50	
31808102	myeloperoxidase	0.52	
3955096	vacuolar proton-translocating ATPase 100 kDa subunit isoform a1	0.56	
16716463	mucolipin 1	0.57	
12835142	vacuolar proton-translocating ATPase 100 kDa subunit isoform a3	0.59	
63652380	ferritin light chain 1	0.60	
14714537	presenilin 2	0.65	
52871	lysosomal acid phosphatase	0.66	
12003982	spinster	0.71	
33126168	peptide/histidine transporter	0.73	
8393510	glucuronidase, beta	0.76	
61555039	flotillin 2	0.76	
21961519	high-affinity copper uptake protein (Slc31a1)	0.78	
12751187	flotillin 1	0.78	
55627734	ribonuclease 6	0.81	
12847813	cathepsin L	0.82	
6753674	dipeptidylpeptidase 4	0.83	
13560695	platelet factor 4	0.84	
31560666	*N*-acetyl galactosaminidase, alpha	0.87	
7442229	acid ceramidase	0.87	
11066228	cathepsin F	0.88	
27369545	osteopetrosis associated transmembrane protein 1	0.88	
227293	cathepsin B	0.89	
55596834	prenylcysteine oxidase 1	0.90	
55732656	legumain	0.91	
35193008	lysosomal acid lipase 1	0.93	
26330552	D8Ertd354e (*N*-acetyltransferase; mouse homologue of human HGSNAT)	0.98	
50852	acrogranin	1.02	
1177440	chloride channel 7	1.16	
4584979	palmitoyl-protein thioesterase	1.18	
	ER		
62739260	Cyp2d9	0.89	
20978509	epoxide hydrolase 1 (Microsomal epoxide hydrolase) (epoxide hydratase)	1.05	
34784803	retinol dehydrogenase 9	1.08	
6753564	Cyp1	1.18	
6806903	ATPase, Ca++ transporting, cardiac muscle, slow twitch 2 isoform 2	1.33	
32822818	arylacetamide deacetylase (esterase)	1.37	
62533207	retinol dehydrogenase 7	1.38	
7430421	very-long-chain acyl-CoA synthetase related protein, solute carrier family 27 (fatty acid transporter), member 5	1.41	
5880468	UDP-glucuronosyltransferase 1A1	1.50	
31982435	Cyp2c29	1.60	
13905188	MOCO sulfurase C-terminal domain containing 2	1.62	
57619220	Cyp4f	1.67	
74213406	dehydrogenase/reductase (SDR family) member 1	1.70	
15488614	Cyp2e1	1.76	
55958189	surfeit 4	1.81	
30046906	Cyp2c50 protein	1.84	
58531102	catechol *O*-methyltransferase	1.86	
14318725	microsomal glutathione *S*-transferase 1	1.87	
46559382	flavin containing monooxygenase 5	1.95	
6679421	NADPH-cytochrome P450 oxidoreductase	2.27	
57107211	Cyp2	3.38	
	Mitochondria		
18034785	ATP-binding cassette, subfamily B (MDR/TAP), member 6	0.77	
5733504	voltage-dependent anion channel VDAC3	0.84	
67971034	ubiquinol-cytochrome *c* reductase core protein 2	0.91	

Table 2 (Continued)

Entrez number	protein name	ratio (Bg/NB)	additional information
	Mitochondria		
38051979	Vdac1 protein	0.93	
21539599	ubiquinol-cytochrome *c* reductase hinge protein	1.01	
483918	glutamate-ammonia ligase	1.10	
62655085	carbamoyl-phosphate synthetase 1	1.16	
729927	long-chain-fatty-acid−CoA ligase 1 (long-chain acyl-CoA synthetase 1) (LACS 1)	1.17	
46593021	ubiquinol-cytochrome *c* reductase core protein 1	1.36	
	Cytosol		
494384	major urinary protein 1	0.56	
50926806	betaine-homocysteine methyltransferase	1.44	
	Extracellular		
56971493	Fibrinogen, beta polypeptide	1.26	
	Cell Surface		
74214302	protein similar to CGI-51	0.45	
7447771	P2X4 receptor	0.59	
13435022	toll-like receptor 3	0.98	
66472876	gap junction membrane channel protein beta 6	1.11	
6680011	gap junction membrane channel protein beta 2 (connexin 26)	1.24	
7656965	CD5 antigen (p56−62)	1.27	
	More Than One Location		
13435930	*N*-ethylmaleimide sensitive fusion protein attachment protein alpha	0.57	golgi, ER
20073042	connexin 32 (gap junction membrane channel protein, beta 1)	0.69	plasma membrane, golgi, lysosome
13096554	Rac1	0.76	
26346446	annexin A7	0.77	phagosome, nuclear
885904	H2-Mb1 beta chain, MHC class II	0.86	ER, lysosome, plasma membrane
3087820	very-long-chain acyl-CoA synthetase (slc27a2)	1.22	ER, plasma membrane, mitochondria, peroxisome
12836373	hydroxysteroid (17-beta) dehydrogenase 4	1.28	mitochondria, peroxidase
199496	MHC H2-I-A-beta chain	1.50	ER, lysosome, plasma membrane
70048	Ig mu chain region, membrane bound form	1.56	
	Unassigned		
22122339	pituitary tumor-transforming gene 1 protein-interacting protein	0.37	
13277735	synaptobrevin like protein 1	0.47	
12832141	apoptosis related protein APR−3 isoform 1	0.51	
12853943	unnamed protein product	0.52	
20071348	Gpr155 protein	0.59	
29835230	SID1 transmembrane family, member 2	0.64	
9910458	kidney predominant protein NCU-G1	0.69	
21703976	dihydroxyacetone kinase 2 homologue	0.73	
7305165	hydroxysteroid (17-beta) dehydrogenase 9	0.81	
51262086	gremlin 2	0.82	
21313266	major facilitator superfamily domain containing 1	0.83	
33469029	acyl-Coenzyme A binding domain containing 3	0.93	
21542264	transmembrane 7 superfamily protein member 3	1.01	
21426871	eosinophil-associated, ribonuclease A family, member 6	1.04	
26333179	BAC30307	1.05	
12857367	PU.1 binding protein Pub	1.17	
57283095	UbiE2	1.34	
12852073	signal peptidase complex subunit 2 homologue	1.38	
27229118	hypothetical protein LOC71664	1.51	
21618729	Acyl-CoA synthetase long-chain family member 5	1.60	
6681251	eosinophil-associated, ribonuclease A family, member 2	1.99	

report that indicated elastase activity was about 32% of normal activity in Beige fibroblasts.[23]

The raw data were searched against Mascot, and only 3 peptides from 2 proteins, that is, 2 peptides for voltage-gated chloride channel 2 and 1 peptide for rab7, were identified without a labeled cysteine. Some soluble lysosomal proteins were also found in the membrane fraction. This likely occurred either because of their high abundance or their propensity for associating with membrane, for example, cathepsin B and L, prenylcysteine oxidase 1, and palmitoyl protein thioesterase 1. It is interesting to note that rat homologues of most of the mouse lysosomal membrane proteins identified in this study were previously identified in a proteomics study of Triton WR-1339-filled membranes from rat liver, an organelle purification method that takes advantage of a different property of lysosomes.[13] The proteins identified by both methods are included in Supplementary Table 3 in Supporting Information. Two proteins of unknown function, that is, a protein similar to CGI-51 and a transmembrane 7 superfamily protein member 3, had been identified in urine exosomes, which come from multivesicular bodies, a specialized form of lysosomes.[24]

The cICAT ratios of Beige lysosomal membrane proteins to normal mouse lysosomal membrane proteins were ordered from low to high and organized according to their generally

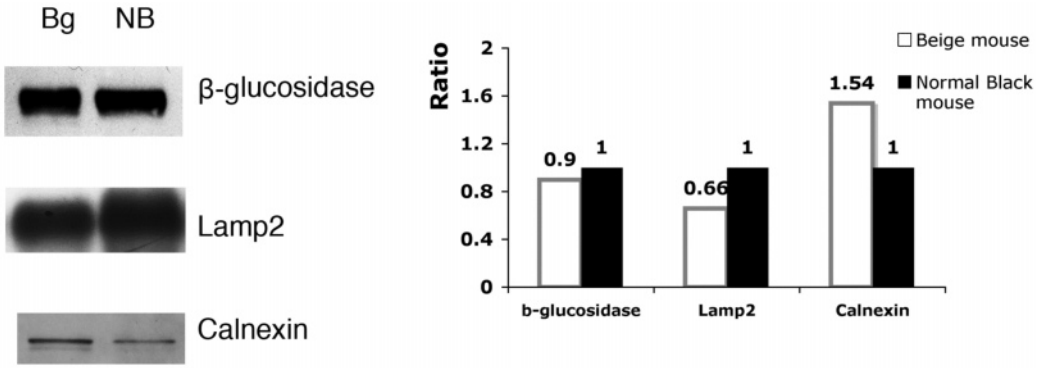

Figure 4. Confirmation of cICAT results by Western blot. Western blot demonstrates that compared to normal (NB), the total Beige lysosomal fraction (Bg) contained relatively more of the ER protein, calnexin, relatively less of the common lysosomal protein Lamp2, and nearly identical amounts of β-glucosidase. For Lamp2, three blots were scanned with an overall Bg/NB ratio of 0.63 $\pm$ 0.02.

accepted intracellular localization (Table 2 and Supplementary Table 2 in Supporting Information). It can readily be seen that the bulk of lysosomal proteins have cICAT ratios (^{13}C Beige/^{12}C normal) from 0.16 to 1.18 (mean $\pm$ SD = 0.69 $\pm$ 0.24, n = 40). For example, the Beige/normal ratios for the recently identified lysosomal proteins Nicastrin (Figure 3D) and Presenilin 2[25] were 0.41 and 0.65, respectively. These values were comparable to the well-recognized lysosomal membrane proteins, for example, Lamp1, 0.40; Lamp2, 0.49; Niemann Pick type C1, 0.50; Mucolipin, 0.57; and lysosomal acid phosphatase, 0.66 (Table 2 and Supplementary Table 2 in Supporting Information).

The relative decrease in the specific levels of lysosomal membrane proteins was accompanied by a relative increase in the specific levels of ER proteins. Ratios for these proteins were in the range from 0.89 to 3.39 with 17/21 having ratios above 1.3. The overall ER distribution ratio was 1.64 $\pm$ 0.52 (mean $\pm$ SD, n = 21), significantly different from the lysosomal protein distribution. Included in this group are several Cytochrome P450 species (Cyp2c29, 1.60; Cyp4f, 1.67; Cyp2e1, 1.76; Cyp2c50, 1.81; Cyp2, 3.38); Glutathione *S*-transferase 1, 1.87; and flavin-containing monooxygenase 5, 1.95 (Table 2). These findings are supported by Basrur et al.[26] who noted the occurrence of several ER proteins including calnexin, calreticulin, and BiP in unfractionated melanosomes from human pigmentary MNT1 cells. The few mitochondrial resident proteins that were identified had ratios in the range of 0.77−1.36, with a 1.03 $\pm$ 0.19 (n = 9) average ratio distribution. Since these mitochondrial proteins may represent contaminants in the lysosomal preparations, the presence of nearly identical amounts of these proteins in both lysosomal fractions confirms the reproducibility between our Beige and normal lysosomal fractionation procedures and can be looked on as internal controls for these cICAT ratios.

To further confirm the above data, we used Western blot to compare the membrane proteins from Beige with those from normal mice (Figure 4). Compared with normal mouse lysosomes, the total of the lysosomal proteins from Beige contained a little less β-glucosidase, far less conventional lysosomal protein Lamp2, and more Calnexin (an ER resident protein). Calnexin was not identified by cICAT, since it does not have cysteine-containing peptides whose m/z values lie in the 350−2000 Da range of our study.

Calnexin Occurs on Human CHS Lysosomes as Patches. We used confocal laser-scanning microscopy to further investigate whether giant lysosomes from CHS patient fibroblasts contain increased levels of ER protein, as compared to lysosomes from normal human fibroblasts. Using an antibody, specific to the N-terminus of Calnexin, we confirmed that, as well as being present in its conventional intracellular ER location, Calnexin was either fully colocalized with Lamp1, or appeared in a patch-like staining pattern on the giant lysosomal membrane decorated with Lamp1 (Figure 5B). It has been previously reported that, after 24 h exposure to colloidal gold, colloidal gold concentrated in foci along the periphery of giant lysosomes.[27] We used dextran, rather than colloidal gold, in our study to chase fluid endocytosis and observed that dextran was primarily localized to small lysosomes and only seen at the side of giant lysosomes under the microscope after cell fixation (Figure 5A).

A consistent, highly enriched lysosomal preparation is the prerequisite for any comparative organelle-specific proteomics study. We achieved this by (i) documenting a ~100-fold enrichment of a lysosomal enzyme (Table 1); (ii) demonstrating a lack of contaminating organelles by Western blots of marker proteins (Figure 1C); (iii) EM analysis (Figure 2A,B), which demonstrated a lack of recognizable contaminating organelles in either the Beige or normal lysosomal fractions; and (iv) additionally showing that the giant lysosomes, characteristic of Beige mice and human CHS patient cells, were enriched in the same manner as normal lysosomes by our procedure. Furthermore, by identifying many soluble proteins in our luminal fractions, we affirm that maturation, for example, proteolytic processing, targeting through the mannose-6-phosphate receptor pathway, and the levels of most soluble lysosomal proteins, are not affected in Beige mice or human CHS patients.[28]

The disproportionate increase in ER proteins in the lysosomal membrane of Beige mice seemingly at the expense of integral lysosomal proteins is novel and intriguing. LYST contains 3801 amino acids where the N-terminal half is dominated by HEAT/ARM repeats and a Perilipin domain, while the C-terminal half contains the BEACH domain (unique to *Be*ige *a*nd *CH*S) and several WD-40 domains of coiled-coil "propeller-like" structures that facilitate protein−protein interactions. Specific roles of each of these domains are poorly understood. McVey Ward and co-workers[29] concluded that LYST had at least 2 separate binding partners, one function of which was to serve as an anchor protein, but the target was unknown, while the other likely involved binding to specific lipids such as phosphatidylinositol 4,5 bisphosphate. The present data suggest that the absence of functional LYST results

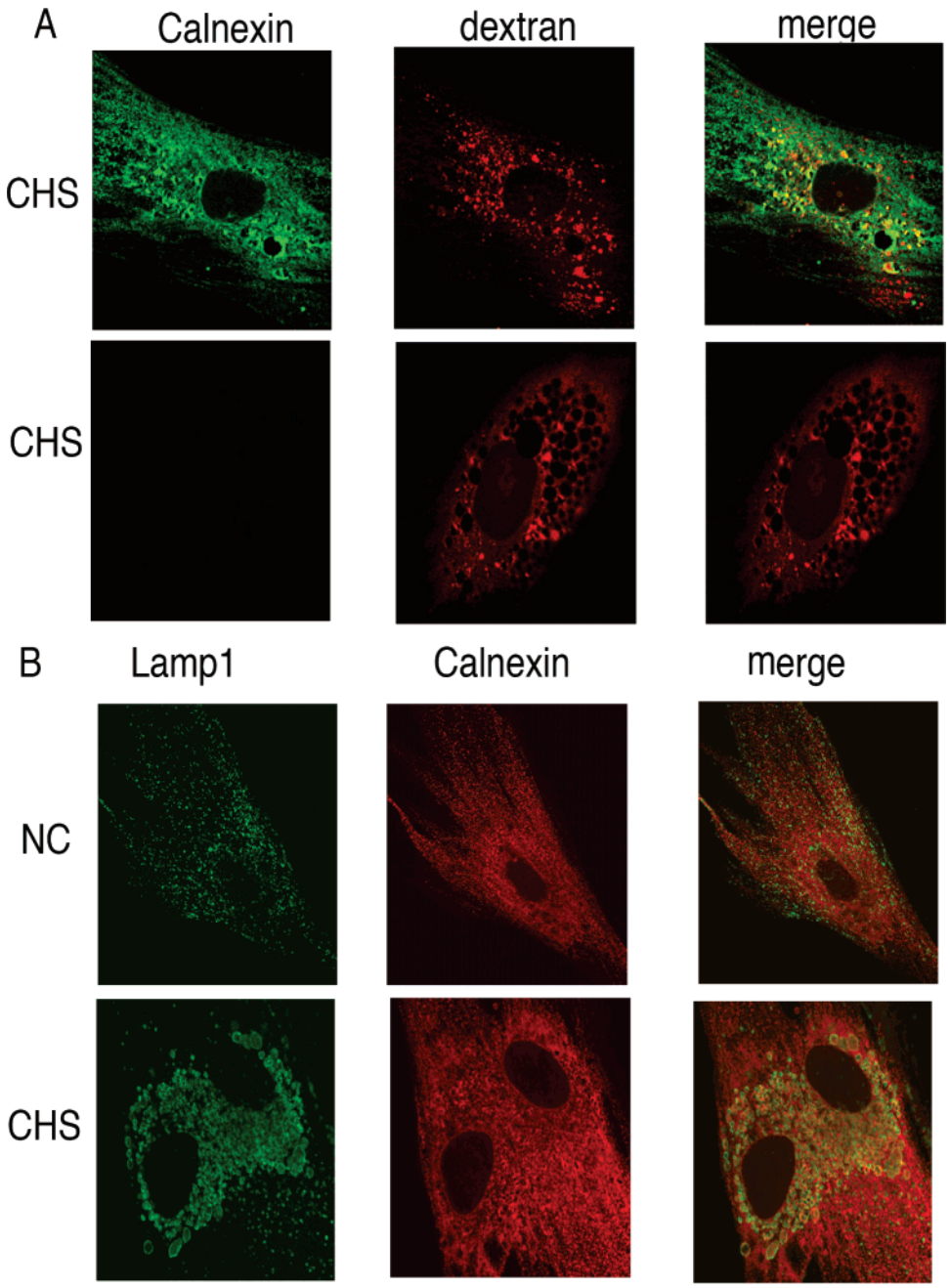

Figure 5. Immunofluorescence showed calnexin as patchy signals on the membrane of giant lysosomes in human CHS fibroblasts. In panels shown under A, CHS fibroblasts were loaded with dextran overnight and chased for 3 h, then labeled with calnexin (H-70) (the first row) or only preimmune rabbit serum (the second row). The images were taken at the same microscope setting. No signal was seen after incubating with the preimmune rabbit serum. In panels shown under B, CHS and normal fibroblasts (NC) were fixed and labeled with antibodies against Lamp1 and calnexin (H-70) simultaneously.

in the stable occurrence of proteins normally considered to be resident ER proteins in the lysosomal membrane. This suggests LYST may play a role in either preventing inappropriate incorporation of these proteins into the lysosomal membrane or in the removal of these elements during recycling/maturation of the lysosomal membrane.

Abbreviations: CHS, Chediak−Higashi syndrome; ER, endoplasmic reticulum; cICAT, cleavable isotope-coded affinity tag technique; LYST, lysosome traffic regulator; Lamp1, lysosome-associated membrane protein.

Acknowledgment. This study was supported by a CIHR (Canadian Institutes of Health Research) grant to J.W.C and D.J.M. We are thankful to Steven Doyle for excellent electron microscopy technique, and Michael Tropak and Sunqu Zhang for inspiring discussions.

Supporting Information Available: Figures showing a flow chart of the purification of lysosomes from mouse liver and the designation of each fraction and two-dimensional electrophoresis of soluble lysosomal proteins; tables listing the proteins identified in the lysosomal soluble fraction, the lysosomal menbrane protein identified by the ICAT technique, and the common proteins identified in the lysosomal membrane by the Percoll and tritosome methods. This material is available free of charge via the Internet at http://pubs.acs.org.

References

(1) Karim, M. A.; Suzuki, K.; Fukai, K.; Oh, J.; Nagle, D. L.; Moore, K. J.; Barbosa, E.; Falik-Borenstein, T.; Filipovich, A.; Ishida, Y.; Kivrikko, S.; Klein, C.; Kreuz, F.; Levin, A.; Miyajima, H.; Regueiro, J.; Russo, C.; Uyama, E.; Vierimaa, O.; Spritz, R. A. Apparent genotype-phenotype correlation in childhood, adolescent, and adult Chediak-Higashi syndrome. *Am. J. Med. Genet.* **2002**, *108* (1), 16−22.

(2) Baetz, K.; Isaaz, S.; Griffiths, G. M. Loss of cytotoxic T lymphocyte function in Chediak-Higashi syndrome arises from a secretory defect that prevents lytic granule exocytosis. *J. Immunol.* **1995**, *154* (11), 6122−6131.

(3) Burkhardt, J. K.; Wiebel, F. A.; Hester, S.; Argon, Y. The giant organelles in beige and Chediak-Higashi fibroblasts are derived from late endosomes and mature lysosomes. *J. Exp. Med.* **1993**, *178* (6), 1845−1856.

(4) Lyons, R. T.; Pitot, H. C. Protein degradation in normal and beige (Chediak-Higashi) mice. *J. Clin. Invest.* **1978**, *61* (2), 260−268.

(5) Perou, C. M.; Leslie, J. D.; Green, W.; Li, L.; Ward, D. M.; Kaplan, J. The Beige/Chediak-Higashi syndrome gene encodes a widely expressed cytosolic protein. *J. Biol. Chem.* **1997**, *272* (47), 29790−29794.

(6) Nagle, D. L.; Karim, M. A.; Woolf, E. A.; Holmgren, L.; Bork, P.; Misumi, D. J.; McGrail, S. H.; Dussault, B. J., Jr.; Perou, C. M.; Boissy, R. E.; Duyk, G. M.; Spritz, R. A.; Moore, K. J. Identification and mutation analysis of the complete gene for Chediak-Higashi syndrome. *Nat. Genet.* **1996**, *14* (3), 307−311.

(7) Cornillon, S.; Dubois, A.; Bruckert, F.; Lefkir, Y.; Marchetti, A.; Benghezal, M.; De Lozanne, A.; Letourneur, F.; Cosson, P. Two members of the beige/CHS (BEACH) family are involved at different stages in the organization of the endocytic pathway in Dictyostelium. *J. Cell Sci.* **2002**, *115* (Pt 4), 737−744.

(8) De Lozanne, A. The role of BEACH proteins in Dictyostelium. *Traffic* **2003**, *4* (1), 6−12.

(9) Simonsen, A.; Birkeland, H. C.; Gillooly, D. J.; Mizushima, N.; Kuma, A.; Yoshimori, T.; Slagsvold, T.; Brech, A.; Stenmark, H. Alfy, a novel FYVE-domain-containing protein associated with protein granules and autophagic membranes. *J. Cell Sci.* **2004**, *117* (Pt 18), 4239−4251.

(10) Faigle, W.; Raposo, G.; Tenza, D.; Pinet, V.; Vogt, A. B.; Kropshofer, H.; Fischer, A.; de Saint-Basile, G.; Amigorena, S. Deficient peptide loading and MHC class II endosomal sorting in a human genetic immunodeficiency disease: the Chediak-Higashi syndrome. *J. Cell Biol.* **1998**, *141* (5), 1121−1134.

(11) Laemmli, U. K. Cleavage, of structural proteins during the assembly of the head of bacteriophage T4. *Nature* **1970**, *227*, 680−685.

(12) Tropak, M. B.; Reid, S. P.; Guiral, M.; Withers, S. G.; Mahuran, D. Pharmacological enhancement of beta-hexosaminidase activity in fibroblasts from adult Tay-Sachs and Sandhoff Patients. *J. Biol. Chem.* **2004**, *279* (14), 13478−13487.

(13) Bagshaw, R. D.; Mahuran, D. J.; Callahan, J. W. A proteomic analysis of lysosomal integral membrane proteins reveals the diverse composition of the organelle. *Mol. Cell. Proteomics* **2005**, *4* (2), 133−143.

(14) Mortz, E.; Krogh, T. N.; Vorum, H.; Gorg, A. Improved silver staining protocols for high sensitivity protein identification using matrix-assisted laser desorption/ionization-time of flight analysis. *Proteomics* **2001**, *1* (11), 1359−1363.

(15) Bagshaw, R. D.; Callahan, J. W.; Mahuran, D. J. Desalting of in-gel-digested protein sample with mini-C18 columns for matrix-assisted laser desorption ionization time of flight peptide mass fingerprinting. *Anal. Biochem.* **2000**, *284* (2), 432−435.

(16) Yamada, H.; Hayashi, H.; Natori, Y. A simple procedure for the isolation of highly purified lysosomes from normal rat liver. *J. Biochem. (Tokyo)* **1984**, *95* (4), 1155−1160.

(17) Kollmann, K.; Mutenda, K. E.; Balleininger, M.; Eckermann, E.; von Figura, K.; Schmidt, B.; Lubke, T. Identification of novel lysosomal matrix proteins by proteome analysis. *Proteomics* **2005**, *5* (15), 3966−3978.

(18) Vergarajauregui, S.; Puertollano, R. Two di-leucine motifs regulate trafficking of mucolipin-1 to lysosomes. *Traffic* **2006**, *7* (3), 337−353.

(19) Sweeney, S. T.; Davis, G. W. Unrestricted synaptic growth in spinster-a late endosomal protein implicated in TGF-beta-mediated synaptic growth regulation. *Neuron* **2002**, *36* (3), 403−416.

(20) Verheijen, F. W.; Verbeek, E.; Aula, N.; Beerens, C. E.; Havelaar, A. C.; Joosse, M.; Peltonen, L.; Aula, P.; Galjaard, H.; van der Spek, P. J.; Mancini, G. M. A new gene, encoding an anion transporter, is mutated in sialic acid storage diseases. *Nat. Genet.* **1999**, *23* (4), 462−465.

(21) Attucci, S.; Korkmaz, B.; Juliano, L.; Hazouard, E.; Girardin, C.; Brillard-Bourdet, M.; Rehault, S.; Anthonioz, P.; Gauthier, F. Measurement of free and membrane-bound cathepsin G in human neutrophils using new sensitive fluorogenic substrates. *Biochem. J.* **2002**, *366* (Pt 3), 965−970.

(22) Benson, K. F.; Li, F. Q.; Person, R. E.; Albani, D.; Duan, Z.; Wechsler, J.; Meade-White, K.; Williams, K.; Acland, G. M.; Niemeyer, G.; Lothrop, C. D.; Horwitz, M. Mutations associated with neutropenia in dogs and humans disrupt intracellular transport of neutrophil elastase. *Nat. Genet.* **2003**, *35* (1), 90−96.

(23) Tanabe, F.; Cui, S. H.; Ito, M. Abnormal down-regulation of PKC is responsible for giant granule formation in fibroblasts from CHS (beige) mice−a thiol proteinase inhibitor, E-64-d, prevents giant granule formation in beige fibroblasts. *J. Leukocyte Biol.* **2000**, *67* (5), 749−755.

(24) Pisitkun, T.; Shen, R. F.; Knepper, M. A. Identification and proteomic profiling of exosomes in human urine. *Proc. Natl. Acad. Sci. U.S.A.* **2004**, *101* (36), 13368−13373.

(25) Bagshaw, R. D.; Pasternak, S. H.; Mahuran, D. J.; Callahan, J. W. Nicastrin is a resident lysosomal membrane protein. *Biochem. Biophys. Res. Commun.* **2003**, *300* (3), 615−618.

(26) Basrur, V.; Yang, F.; Kushimoto, T.; Higashimoto, Y.; Yasumoto, K.; Valencia, J.; Muller, J.; Vieira, W. D.; Watabe, H.; Shabanowitz, J.; Hearing, V. J.; Hunt, D. F.; Appella, E. Proteomic analysis of early melanosomes: identification of novel melanosomal proteins. *J. Proteome Res.* **2003**, *2* (1), 69−79.

(27) Vincent, R. A., Jr.; Spicer, S. S. Giant dense bodies in fibroblasts cultured from beige mice with the Chediak-Higashi syndrome. *Am. J. Pathol.* **1981**, *105* (3), 270−278.

(28) Stinchcombe, J. C.; Page, L. J.; Griffiths, G. M. Secretory lysosome biogenesis in cytotoxic T lymphocytes from normal and Chediak Higashi syndrome patients. *Traffic* **2000**, *1* (5), 435−444.

(29) McVey Ward, D.; Shiflett, S. L.; Huynh, D.; Vaughn, M. B.; Prestwich, G.; Kaplan, J. Use of expression constructs to dissect the functional domains of the CHS/Beige protein: identification of multiple phenotypes. *Traffic* **2003**, *4*, 403−415.

PR060407O